

# Measuring Distance between Reeb Graphs

[Extended abstract]

Ulrich Bauer  
IST Austria  
Klosterneuburg, Austria  
mail@ulrich-bauer.org

Xiaoyin Ge  
The Ohio State University  
Columbus, OH, USA  
gex@cse.ohio-state.edu

Yusu Wang  
The Ohio State University  
Columbus, OH, USA  
yusu@cse.ohio-state.edu

## ABSTRACT

We propose a metric for Reeb graphs, called the functional distortion distance. Under this distance, the Reeb graph is stable against small changes of input functions. At the same time, it remains discriminative at differentiating input functions. In particular, the main result is that the functional distortion distance between two Reeb graphs is bounded from below by the bottleneck distance between both the ordinary and extended persistence diagrams for appropriate dimensions.

As an application of our results, we analyze a natural simplification scheme for Reeb graphs, and show that persistent features in Reeb graph remains persistent under simplification. Understanding the stability of important features of the Reeb graph under simplification is an interesting problem on its own right, and critical to the practical usage of Reeb graphs.

## 1. INTRODUCTION

One of the prevailing ideas in geometric and topological data analysis is to provide descriptors that encode useful information about hidden objects from observed data. The Reeb graph is one such descriptor. Specifically, given a continuous function  $f : X \rightarrow \mathbb{R}$  defined on a domain  $X$ , the levelset of  $f$  at value  $a$  is the set  $f^{-1}(a) = \{x \in X \mid f(x) = a\}$ . As the scalar value  $a$  increases, connected components appear, disappear, split and merge in the level set, and the Reeb graph of  $f$  tracks such changes. It provides a simple yet meaningful abstraction of the input domain. The concept behind the Reeb graph was first introduced in [30]. The term Reeb graph was made by R. Thom and first used for shape understanding by Shinagawa et al. [31]. Since then, it has been used in a variety of applications in graphics and visualization, e.g. [23, 24, 27, 31, 33, 35]; also see [5] for a survey.

The Reeb graph can be computed efficiently in  $O(m \log m)$  time for a piecewise-linear function defined on an arbitrary simplicial complex domain with  $m$  vertices, edges and triangles [28] (a randomized algorithm was given in [21]). This is in contrast to, for example, the  $O(m^3)$  time (or matrix multiplication time) needed to compute even just the first-dimensional homology information for the same simplicial complex. The Reeb graph of a scalar field on a manifold

Permission to make digital or hard copies of all or part of this work for personal or classroom use is granted without fee provided that copies are not made or distributed for profit or commercial advantage and that copies bear this notice and the full citation on the first page. Copyrights for components of this work owned by others than the author(s) must be honored. Abstracting with credit is permitted. To copy otherwise, or republish, to post on servers or to redistribute to lists, requires prior specific permission and/or a fee. Request permissions from Permissions@acm.org.

*SoCG'14*, June 8–11, 2014, Kyoto, Japan.

Copyright is held by the owner/author(s). Publication rights licensed to ACM. ACM 978-1-4503-2594-3/14/06 ...\$15.00.

can also be approximated from a point sample efficiently and with theoretical guarantees [15]. It encodes meaningful information on the input scalar field, in particular the so-called one-dimensional *vertical homology group* [15]. Being a graph structure, the Reeb graph is simple to represent and manipulate. These properties make the Reeb graph appealing for analyzing high-dimensional point data. For example, a generalization of the Reeb graph is proposed in [32] for analyzing high dimensional data, and in [20], the Reeb graph is used to recover a hidden geometric graph from its point samples. Very recently in [9], it is shown that a certain Reeb graph can reconstruct a metric graph with respect to the Gromov-Hausdorff distance.

Given the popularity of the Reeb graph in data analysis, it is important to understand its stability and robustness with respect to changes in the input function (both in function values and in the domain). To measure the stability, we first need to define a distance between two Reeb graphs. Furthermore, an important application of the Reeb graph is to provide a descriptive summary of the function. Again, a central problem involved is to have a meaningful distance between Reeb graphs.

In this paper, we propose a metric for Reeb graphs, called the *functional distortion distance*, drawing intuition from the Gromov-Hausdorff distance for measuring metric distortion. Under this distance, the Reeb graph is stable against perturbations of the input function; at the same time, it retains a certain ability to discriminate between different functions (these statements will be made precise in Section 4). In particular, the main result is that the functional distortion distance between two Reeb graphs is bounded from below by (and thus more discriminative than) the *bottleneck distance* between the persistence diagrams of the Reeb graphs. On the other hand, the functional distortion distance yields the same type of sup norm stability that persistence diagrams enjoy [2, 10, 12, 13]. The persistence diagram has been a popular topological summary of shapes and functions, and the bottleneck distance is introduced in [13] as a natural distance for persistence diagrams. However, as the simple example in Fig. 1 (a) shows, the Reeb graph can be strictly more discriminative than the persistence diagram of dimension 0.

As an application of our results, we show in Section 5 that persistent features of the Reeb graph remain persistent under a certain natural simplification strategy of the Reeb graph.

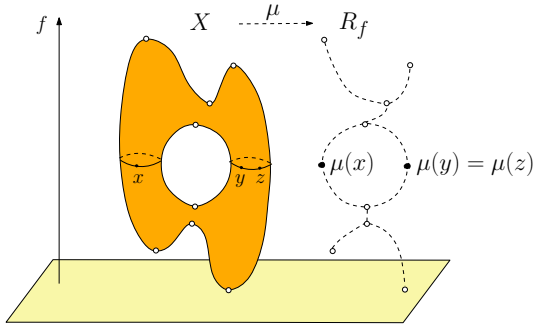
In the special case of Reeb graphs of functions on curves, similar results were obtained in [17] using an editing distance on Reeb graphs, and this approach is being extended to surfaces by the same authors. Recently, Morozov et al. proposed the *interleaving distance* for *merge trees*, based on the concept of an interleaving [10], and obtained similar upper and lower bounds relating this distance to *ordinary* persistence diagrams [26]. Here, the merge trees are variants of the loop-free Reeb graphs (*contour trees*). However, it is not clear

how to generalize these results to Reeb graphs containing loops, an important family of features of the Reeb graph. Another distance based on the *branch decomposition* of merge trees was proposed in [4], together with a polynomial time algorithm to compute it. This distance, however, is not stable with respect to changes in the function and also does not generalize beyond trees.

Details omitted from this extended abstract can be found in [3].

## 2. PRELIMINARIES AND PROBLEM DEFINITION

**Reeb graphs.** Given a continuous function  $f : X \rightarrow \mathbb{R}$  on a finitely triangulable topological space  $X$ , for each  $a \in \mathbb{R}$ , the set  $f^{-1}(a) = \{x \in X : f(x) = a\}$  is called a *level set* of  $f$ . A level set may consist of several connected components. We define an equivalence relation  $\sim$  on  $X$  such that  $x \sim y$  iff  $f(x) = f(y) = a$  and  $x$  is connected to  $y$  in  $f^{-1}(a)$ . The *Reeb space* of the function



$f : X \rightarrow \mathbb{R}$ , denoted by  $R_f$ , is the quotient space  $X/\sim$ , i.e., the set of equivalent classes equipped with the quotient topology induced by the quotient map  $\mu : X \rightarrow R_f$ . Under appropriate regularity assumptions (to be made precise later),  $R_f$  has the structure of a finite 1-dimensional regular CW complex, and we call it a *Reeb graph*. Throughout this paper, we tacitly assume that all mentioned connected components are also path-connected.

The input function  $f : X \rightarrow \mathbb{R}$  also induces a continuous function  $\tilde{f} : R_f \rightarrow \mathbb{R}$  defined as  $\tilde{f}(z) = f(x)$  for any preimage  $x \in \mu^{-1}(z)$  of  $z$ . To simplify notation, we often write  $f(z)$  instead of  $\tilde{f}(z)$  for  $z \in R_f$  when there is no ambiguity, and use  $\tilde{f}$  mostly to emphasize the different domains of the functions. In all illustrations of this paper, we plot the Reeb graph with the vertical coordinate of a point  $z$  corresponding to the function value  $f(z)$ .

Given a point  $x \in R_f$ , we use the term *up-degree* (resp. *down-degree*) of  $x$  to denote the number of branches (1-cells) incident to  $x$  that have higher (resp. lower) values of  $f$  than  $x$ . A point is *regular* if both of its up-degree and down-degree equal to 1, and *critical* otherwise. A critical point is a minimum (maximum) if it has down-degree 0 (up-degree 0), and a down-fork (up-fork) if it has down-degree (up-degree) larger than 1. A critical point can be degenerate, having more than one types of criticality. From now on, we use the term *node* to refer to a critical point in the Reeb graph. For simplicity of exposition, we assume that all nodes of the Reeb graph have distinct  $\tilde{f}$  function values. Note that because of the monotonicity of  $\tilde{f}$  at regular points, the Reeb graph together with its associated function is completely described, up to homeomorphisms preserving the function, by the function values on the nodes.

**Persistent homology and persistence diagrams.** The notion of persistence was originally introduced by Edelsbrunner et al. in [19]. There has since been a great amount of development both in theory and in applications; see, e.g., [2, 7, 12, 36]. This paper does not

concern the theory of persistence, hence we only provide a simple description so as to introduce the notion of *persistence diagrams*, which will be used later. We refer the readers to [22] for a detailed treatment of homology groups in general and to [18] for persistent homology.

Given a continuous function  $f : X \rightarrow \mathbb{R}$  defined on a finitely triangulable topological space  $X$ , we call  $X_{\leq a} = \{x \in X \mid f(x) \leq a\}$  a *sublevel set* of  $f$ . Let  $H_p(Y)$  denote the  $p$ -th homology group of a triangulable topological space  $Y$ . Recall that a triangulation gives a CW structure and singular, simplicial, and cellular homology are isomorphic (see [22] for details). In this paper, we always consider homology with coefficients in  $\mathbb{Z}_2$ , so  $H_p(Y)$  is a vector space. We now investigate the changes of  $H_p(X_{\leq a})$  for increasing values of  $a$ . Throughout this paper, we will assume that  $f$  is *tame* in the following sense: there is a finite partition  $-\infty = a_0 < \min f = a_1 < \dots < a_N = \max f < \infty = a_{N+1}$  such that for all  $i < n$  and  $s, t \in [a_i, a_{i+1}]$  with  $s < t$ , the homomorphism  $H_p(X_{\leq s}) \rightarrow H_p(X_{\leq t})$  induced by the inclusion  $X_{\leq s} \hookrightarrow X_{\leq t}$  is an isomorphism, and similarly, for all  $s, t \in (a_i, a_{i+1})$  with  $s < t$ , the homomorphism  $H_p(X_{\geq t}) \rightarrow H_p(X_{\geq s})$  induced by the inclusion  $X_{\geq t} \hookrightarrow X_{\geq s}$  is an isomorphism. Moreover,  $H_p(X_{\leq a_i}) < \infty$  for all  $i$ . This implies that  $R_f$  is a Reeb graph. We call  $a_i$  a *homologically critical level* of  $f$ .

Consider the following sequence of vector spaces,

$$0 = H_p(X_{\leq a_0}) \rightarrow H_p(X_{\leq a_1}) \rightarrow \dots \rightarrow H_p(X_{\leq a_N}) = H_p(X), \quad (1)$$

where each homomorphism  $\mu_i^j : H_p(X_{\leq a_i}) \rightarrow H_p(X_{\leq a_j})$  is induced by the canonical inclusion  $X_{\leq a_i} \hookrightarrow X_{\leq a_j}$ .

A homology class  $h$  is created at  $a_i$  if

$$h \in H_p(X_{\leq a_i}) \text{ but } h \notin \text{im } \mu_{i-1}^i.$$

It is destroyed at  $a_j$  if

$$\mu_i^{j-1}(h) \notin \text{im } \mu_{i-1}^{j-1} \text{ but } \mu_i^j(h) \in \text{im } \mu_{i-1}^j.$$

Persistent homology records such birth and death events. In particular, the  $p$ -th *ordinary persistence diagram* of  $f$ , denoted by  $Dg_p(f)$ , is a multiset of pairs  $(b, d)$  corresponding to the birth value  $b$  and death value  $d$  of some  $p$ -dimensional homology class. See Figure 1 (c) for an example of the 0-th persistence diagram. (We note that this is only an intuitive and informal introduction of the persistence diagram; see [18, 36] for a more formal treatment.)

In general, since  $H_p(X)$  may not be trivial, any nontrivial homology class of  $H_p(X)$ , referred to as an *essential homology class*, will never die during the sequence in Eq. (1). For example, there is a point  $(a_1, \infty)$  in Fig. 1 (b) indicating a 0-dimensional homology class that was created at  $a_1$  but never dies. By appending a sequence of relative homology groups to Eq. (1), we obtain a pairing of the essential homology classes (i.e., homology classes of  $H_p(X)$ ):

$$0 = H_p(X_{\leq a_0}) \rightarrow \dots \rightarrow H_p(X_{\leq a_N}) = H_p(X) = \\ H_p(X, X_{\geq a_N}) \rightarrow H_p(X, X_{\geq a_{N-1}}) \rightarrow \dots \rightarrow H_p(X, X_{\geq a_0}) = 0. \quad (2)$$

Here  $X_{\geq a}$  denotes the *superlevel set*  $X_{\geq a} = \{x \in X \mid f(x) \geq a\}$ . Since the last vector space  $H_p(X, X_{\geq a_0}) = 0$ , each essential homology class will necessarily die in the *relative part* of the above sequence at some relative homology group  $H_p(X, X_{\geq a_j})$ . We refer to the multiset of points encoding the birth and death time of  $p$ th homology classes created in the ordinary part and destroyed in the relative part of the sequence in Eq. (2) as the  *$p$ th extended persistence diagram* of  $f$ , denoted by  $ExDg_p(f)$ . In particular, for each point  $(b, d)$  in  $ExDg_p(f)$  there is a (essential) homology class in  $H_p(X)$  that is born in  $H_p(X_{\leq b})$  and dies at  $H_p(X, X_{\geq d})$ . See Fig. 1 (d) for an example;

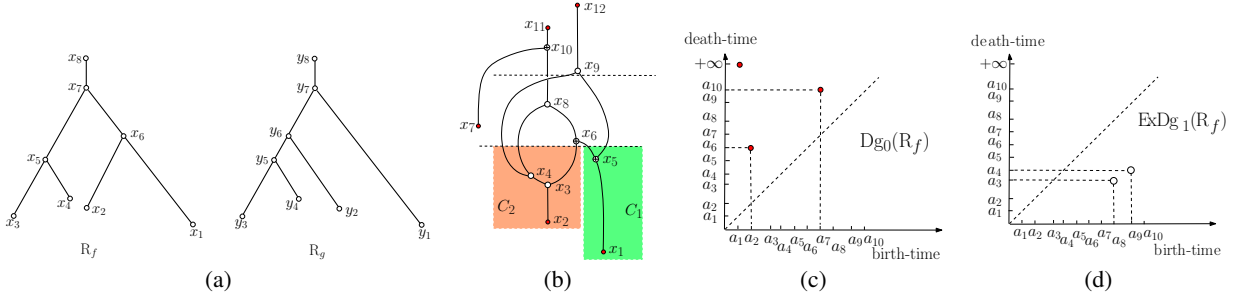


**Figure 1:** (a) The height functions on the two trees have the same persistence diagrams (thus the bottleneck distance between their persistence diagrams is 0), but their tree structures are different. The functional distortion distance will differentiate these two cases. In (b), solid dots are minimum and maximum, empty dots are essential forks, and crossed-dots are ordinary forks. The ordinary fork  $x_6$  merges components  $C_1$  and  $C_2$  in the sublevel set below it, represented by minima  $x_1$  and  $x_2$  respectively. The resulting critical pair  $(x_2, x_6)$  gives rise to the point  $(a_2, a_6)$  in  $Dg_0(R_f)$  in (c), where  $a_i = f(x_i)$  for  $i \in [1, 12]$ . The essential fork  $x_9$  is paired with the up-fork  $x_4$ , corresponding to the thin loop  $x_4 x_8 x_5 x_9 x_4$  created at  $x_9$ . This gives rise to the point  $(a_4, a_9)$  in the extended persistence diagram  $ExDg_1(R_f)$  in (d).

note that the birth time is larger than or equal to death time in the extended persistence diagram.

**Reeb graphs and persistent homology.** There is a natural way to define and quantify features of the Reeb graph, which turns out to be consistent with the information encoded in the diagrams  $Dg_0(R_f)$  and  $ExDg_1(R_f)$  of the function  $\tilde{f} : R_f \rightarrow \mathbb{R}$ . Since  $R_f$  is a graph, we only need to consider persistent homology in dimensions 0 and 1. We provide an intuitive treatment below. For simplicity of exposition, we assume that all nodes have different function values and are either a minimum, a maximum, a down-fork with down-degree 2, or an up-fork with up-degree 2, noting that these assumptions hold in the generic case.

Imagine that we sweep through  $R_f$  in increasing values of  $a$  and inspect changes in  $H_0((R_f)_{\leq a})$ . New components in the *sublevel sets* are created at minima of  $R_f$ . For any value  $a$ , associate each component  $C$  in the sublevel set of  $(R_f)_{\leq a}$  with the lowest local minimum  $m$  contained in  $C$ : intuitively,  $C$  is created at  $m$ .

Consider a down-fork node  $s$  with  $a = f(s)$ . If the two lower branches are contained in different connected components  $C_1$  and  $C_2$  of the open sublevel set  $(R_f)_{< a}$ , for reasons that will become obvious soon we call  $s$  an *ordinary fork*; otherwise, it is an *essential fork*. Let  $x_1$  and  $x_2$  be the global minimum of  $C_1$  and  $C_2$ , respectively. Assume that  $f(x_1) < f(x_2)$ . Then the homology class  $[x_2 + x_1]$  is created at  $f(x_2)$  and dies at  $f(s)$ , giving rise to a unique point  $(f(x_2), f(s))$  in the 0-th ordinary persistence diagram  $Dg_0(R_f)$ . Indeed, there is a one-to-one correspondence between the set of such pairs of minima and ordinary down-forks and points in the 0th persistence diagram  $Dg_0(R_f)$  with finite coordinates; see Fig. 1 (b) and (c). A symmetric procedure with  $-f$  will produce pairs of maxima and ordinary up-forks, corresponding to points in the 0th persistence diagram  $Dg_0(R_f)$ . Together, these pairs capture the *branching features* of a Reeb graph.

If, on the other hand, the two lower branches of  $s$  are connected in the sublevel set, we call  $s$  an *essential fork*; see Fig. 1 (b) and (d). In this case, some cellular 1-cycle in the sublevel set  $(R_f)_{\leq a}$  is born at  $a$ . Since  $R_f$  is a graph, this cycle is non-trivial in  $R_f$ , and their corresponding homology classes will not be destroyed in ordinary persistent homology. Consider the unique cycle  $\gamma$  with largest minimum value of  $f$  among all cycles born at  $a$  and corresponding to an embedded loop in  $R_f$ . Let  $s'$  be the point achieving the minimum on  $\gamma$ . Then the cycle  $\gamma$  is created at  $f(s')$  during the ordinary sequence of Eq. (2), and killed at time  $f(s')$  in the extended part, giving rise to a unique point  $(\tilde{f}(s'), \tilde{f}(s))$  in the 1st extended persistence diagram of  $\tilde{f}$ . It turns out that  $s'$  is necessarily an essential up-fork [1],

and we call such a pair  $(s', s)$  an *essential pair*. Indeed, the collection of essential pairs has a one-to-one correspondence to points in  $ExDg_1(R_f)$ . (The extended persistence diagram  $ExDg_1(R_f)$  is the reflection of  $ExDg_1(R_f)$  and thus encodes the same information as  $ExDg_1(R_f)$ .) These essential pairs capture the *cycle features* of a Reeb graph.

In short, the branching features and cycle features of a Reeb graph give rise to points in the 0th ordinary and 1st extended persistence diagrams, respectively. However, the persistence diagram captures only the lifetime of features, but not how these features are connected; see Fig. 1 (a). In this paper we aim to develop a way of measuring distance between Reeb graphs which also takes into account the graph structure.

### 3. A METRIC ON REEB GRAPHS

Throughout this paper, by a *distance* we will mean an extended pseudometric, i.e., a binary symmetric function  $d$  with values in  $[0, \infty]$  that satisfies  $d(x, x) = 0$  and  $d(x, z) \leq d(x, y) + d(y, z)$ . From now on, consider two Reeb graphs  $R_f$  and  $R_g$ , generated by tame functions  $f : X \rightarrow \mathbb{R}$  and  $g : Y \rightarrow \mathbb{R}$ . While topologically each Reeb graph is simply a 1-dimensional regular CW complex, it is important to note that it also has a function associated with it (induced from the input scalar field). Hence the distance should depend on both the graph structures and the functions  $\tilde{f}$  and  $\tilde{g}$ . Approaching the problem through graph isomorphisms does not seem viable, as small perturbation of the function  $f$  may create an arbitrary number of new branches and loops in the graph. To this end, we first put the following metric structure on a Reeb graph  $R_f$  to capture information about the function  $f$ .

Specifically, for any two points  $u, v \in R_f$  (not necessarily nodes), let  $\pi$  be a continuous path between  $u$  and  $v$ . The *range* of this path is the interval  $\text{range}(\pi) := [\min_{x \in \pi} f(x), \max_{x \in \pi} f(x)]$ , and its *height* is simply the length of the range, denoted by  $\text{height}(\pi) = \max_{x \in \pi} f(x) - \min_{x \in \pi} f(x)$ . We define the distance

$$d_f(u, v) = \min_{\pi: u \sim v} \text{height}(\pi), \quad (3)$$

where  $\pi$  ranges over all paths from  $u$  to  $v$ , denoted by  $u \sim v$ . Equivalently,  $d_f(u, v)$  is the minimum length of any interval  $I$  such that  $u$  and  $v$  are in the same connected component of  $f^{-1}(I)$ . Note that this is in fact a metric, since on Reeb graphs there is no path of constant function value between two points  $u \neq v$ . We put  $f$  in the subscript to emphasize the dependency on the input function. Intuitively,  $d_f(u, v)$  is the minimal function difference one has to overcome to move from  $u$  to  $v$ .

To define a distance between  $R_f$  and  $R_g$ , we need to connect the spaces  $R_f$  and  $R_g$ , which is achieved by continuous maps  $\phi : R_f \rightarrow R_g$  and  $\psi : R_g \rightarrow R_f$ . Borrowing from the definition of Gromov–Hausdorff distance given in [25], let

$$G(\phi, \psi) = \{(x, \phi(x)) : x \in R_f\} \cup \{(\psi(y), y) : y \in R_g\} \text{ and}$$

$$D(\phi, \psi) = \sup_{(x,y), (\tilde{x},\tilde{y}) \in G(\phi,\psi)} \frac{1}{2} |d_f(x, \tilde{x}) - d_g(y, \tilde{y})|, \quad (4)$$

where  $G(\phi, \psi)$ , the union of the graphs of  $\phi$  and  $\psi$ , can be thought of as the set of correspondences between  $R_f$  and  $R_g$  induced by maps  $\phi$  and  $\psi$ . The *functional distortion distance* is defined as:

$$d_{FD}(R_f, R_g) = \inf_{\phi, \psi} \max \{D(\phi, \psi), \|f - g \circ \phi\|_\infty, \|f \circ \psi - g\|_\infty\}, \quad (5)$$

where  $\phi$  and  $\psi$  range over all continuous maps between  $R_f$  and  $R_g$ . The latter two terms address the fact that composition with isometries of the real line (translation, negation) do not affect the metric  $d_f$  induced by a function  $f$ . Note that this definition can be considered as a continuous, functional variant of the Gromov–Hausdorff distance, with the additional condition that the maps between  $R_f$  and  $R_g$  are required to be continuous, and taking into consideration the difference between the function values of corresponding points as well. In fact, this definition is the continuous version of the extended Gromov–Hausdorff distance introduced in Definition 2.4 of [11]. Furthermore, it turns out that for metric graphs, our continuous version of the extended Gromov–Hausdorff (GH) distance is a constant factor approximation of the extended GH distance induced by arbitrary maps; see [3] for details. As an example, consider the two trees in Fig. 1. The distortion of distances in the two trees in (a) is large no matter how we identify correspondences between points from them. Thus the functional distortion distance between them is also large, making it more discriminative than the bottleneck distance between persistence diagrams.

It is straightforward to show that the functional distortion distance is a pseudometric, and a metric on the equivalence classes of Reeb graphs up to function-preserving homeomorphisms. Note that this definition and our results apply to any graph  $G$  with a function  $f$  that is strictly monotonic on the edges. This is easy to see since in that case  $R_f = G$  and  $\tilde{f} = f$ .

## 4. PROPERTIES OF THE FUNCTIONAL DISTORTION DISTANCE

In this section, we show that the functional distortion distance is both stable (upper bounded) and discriminative (lower bounded). Note that it is somewhat meaningless to discuss the stability of a distance alone without understanding its discriminative power – the constant function with value 0 is a pseudo-metric too.

### 4.1 Stability and Relation to Ordinary Persistence Diagram

Suppose that  $f$  and  $g$  are defined on the same domain  $X$ . Furthermore, assume that the quotient maps  $\mu_f$  and  $\mu_g$  have continuous sections (right-inverses)  $s_f$  and  $s_g$ , i.e.,  $\mu_f \circ s_f = \text{id}_{R_f}$  and  $\mu_g \circ s_g = \text{id}_{R_g}$ . Then we have the following stability result for the metric  $d_{FD}$  for Reeb graphs.

**THEOREM 4.1.** *Let  $f, g : X \rightarrow \mathbb{R}$  be tame functions whose Reeb quotient maps  $\mu_f : X \rightarrow R_f$  and  $\mu_g : X \rightarrow R_g$  have continuous sections. Then  $d_{FD}(R_f, R_g) \leq \|f - g\|_\infty$ .*

**PROOF.** Let  $\delta = \|f - g\|_\infty$ . Choose  $\phi = \mu_g \circ s_f, \psi = \mu_f \circ s_g$ . Now assume that  $(x, y), (\tilde{x}, \tilde{y}) \in G(\phi, \psi)$ , with  $G(\phi, \psi)$  as defined in (4).

Let  $\xi = s_f(x), \tilde{\xi} = s_f(\tilde{x}), \nu = s_g(y)$ , and  $\tilde{\nu} = s_g(\tilde{y})$ . Note that either  $y = \phi(x)$  or  $x = \psi(y)$ , so either

$$\mu_g(\nu) = y = \phi(x) = \mu_g \circ s_f(x) = \mu_g(\xi)$$

or

$$\mu_f(\xi) = x = \psi(y) = \mu_f \circ s_g(y) = \mu_f(\nu).$$

In other words,  $\xi$  and  $\nu$  are either in the same level set of  $f$  or of  $g$ , and analogously for  $\tilde{\xi}$  and  $\tilde{\nu}$ .

Let  $[a, b]$  be such that  $x, \tilde{x}$  are connected in  $\tilde{f}^{-1}[a, b]$ . Then  $\xi$  and  $\tilde{\xi}$  are connected in  $f^{-1}[a, b] \subset g^{-1}[a - \delta, b + \delta]$ , and hence, by the above, so are  $\nu$  and  $\tilde{\nu}$ . Therefore,  $y$  and  $\tilde{y}$  are connected in  $\tilde{g}^{-1}[a - \delta, b + \delta]$ . We conclude that  $(b - a) + 2\delta \geq d_g(y, \tilde{y})$ . Since this inequality holds for all intervals  $[a, b]$  with the stated properties, we have  $d_f(x, \tilde{x}) + 2\delta \geq d_g(y, \tilde{y})$ . By symmetry of the above argument, we also have  $d_g(y, \tilde{y}) + 2\delta \geq d_f(x, \tilde{x})$ . Moreover, by assumption,  $\max_{x \in R_f} |f(x) - g(\phi(x))| \leq \max_{y \in X} |f(y) - g(y)| = \delta$ . Similarly,  $\max_{x \in R_g} |g(x) - f(\psi(x))| \leq \max_{y \in X} |g(y) - f(y)| = \delta$ . Hence  $\|f - g \circ \phi\|_\infty \leq \delta$  and  $\|f \circ \psi - g\|_\infty \leq \delta$ . Combining these with (5), we conclude that  $d_{FD}(R_f, R_g) \leq \|f - g\|_\infty$ .  $\square$

The above result is similar to the stability result obtained for the bottleneck distance between persistence diagrams [14], as well as for the  $\epsilon$ -interleaving distance between merge trees [26]. Note that the above stated conditions are only required for the stability result. They are not necessary for Theorems 4.2 and 4.3. The condition on the common domain  $X$  is required so that we can define the distance between input scalar fields  $f$  and  $g$ . The condition on the existence of sections is purely technical; it holds e.g. for Morse functions or for generic PL functions.

The main part of this section is devoted to discussing the discriminative power of the functional distortion distance for Reeb graphs. In particular, we relate this distance with the bottleneck distance between persistence diagrams. We have already seen in Fig. 1 (a) that there are cases where the functional distortion distance is strictly larger than the bottleneck distance between persistence diagrams of according dimensions (0th ordinary and 1st extended persistence diagrams). We next show that, up to a constant factor, the functional distortion distance is always at least as large as the bottleneck distance. As discussed in Section 4.3, we take different approaches to investigate the branching features (ordinary persistence diagram) and the cycle features (extended persistence diagram). For the former, we have the following main result. The proof is rather standard, and similar to the result on interleaving distance between merge trees in [26].

**THEOREM 4.2.**  *$d_B(Dg_0(R_f), Dg_0(R_g)) \leq d_{FD}(R_f, R_g)$ . Similarly,  $d_B(Dg_0(R_{-f}), Dg_0(R_{-g})) \leq d_{FD}(R_f, R_g)$ .*

**PROOF.** Let  $\phi : R_f \rightarrow R_g$  and  $\psi : R_g \rightarrow R_f$  be the optimal continuous maps that achieve  $\delta = d_{FD}(R_f, R_g)$ <sup>1</sup>. First, note that by Eq. (5),  $\max_{x \in R_f} |f(x) - g(\phi(x))| \leq \delta$ . Hence  $\phi : (R_f)_{\leq \alpha} \rightarrow (R_g)_{\leq \alpha + \delta}$  is well defined for any  $\alpha \in \mathbb{R}$ . Similarly,  $\psi : (R_g)_{\leq \beta} \rightarrow (R_f)_{\leq \beta + \delta}$  is well defined for any  $\beta \in \mathbb{R}$ . Hence maps in the left diagram below are well-defined. Let  $i$  denote the canonical inclusion maps, and for any map  $\rho$ , let  $\rho_*$  indicate the induced homomorphism on homology. We now show that the following diagram commutes for any real

<sup>1</sup>If the  $d_{FD}(R_f, R_g)$  is achieved only in the limit, then one can extend the argument by constructing two sequences of maps that are optimal up to an arbitrarily small additive term  $\epsilon$  and taking the limit in the distance they induce.

values  $\alpha$ :

$$\begin{array}{ccc} H_0((R_f)_{\leq \alpha}) & \xrightarrow{i_*} & H_0((R_f)_{\leq \alpha+2\delta}) \\ & \searrow \phi_* & \nearrow \psi_* \\ & H_0((R_g)_{\leq \alpha+\delta}) & \end{array}$$

To show the commutativity of the above diagram, we need to show that for any 0-cycle  $c$  in  $(R_f)_{\leq \alpha}$ ,  $[i(c)] = [\psi \circ \phi(c)]$ , where  $[c']$  is the homology class represented by a cycle  $c'$ . Assume w.l.o.g. that the 0-cycle  $c = x_1 + x_2$  contains only two points  $x_1, x_2$  from  $(R_f)_{\leq \alpha}$ ; the argument easily extends to the case where  $c$  contains an arbitrary even number of points. Let  $x'_1 = \psi \circ \phi(x_1)$  and  $x'_2 = \psi \circ \phi(x_2)$ . Since  $d_f(x_1, x'_1) \leq \delta$ , we know that there is a path (1-chain)  $\pi(x_1, x'_1)$  with height at most  $\delta$  connecting  $x_1$  and  $x'_1$ . In other words,  $x_1$  and  $x'_1$  are connected in  $(R_f)_{\leq \alpha+\delta} \subseteq (R_f)_{\leq \alpha+2\delta}$ . Similarly,  $x_2$  and  $x'_2$  are connected in  $(R_f)_{\leq \alpha+2\delta}$ . Hence the new 0-cycle  $c' = x'_1 + x'_2 = \psi \circ \phi(c)$  is homologous to  $c$  in  $(R_f)_{\leq \alpha+2\delta}$ . Thus,  $[i(c)] = [c'] = [\psi \circ \phi(c)]$ .

A similar argument also shows that the symmetric versions of the diagrams in Section 4.1 (by switching the roles of  $R_f$  and  $R_g$ ) also commute at the 0th homology level. This means that the two persistence modules  $\{H_0((R_f)_{\leq \alpha})\}_\alpha$  and  $\{H_0((R_g)_{\leq \beta})\}_\beta$  are strongly  $\delta$ -interleaved (as introduced in [10]). The first half of Theorem 4.2 then follows from Theorem 4.8 of [10].

The same argument works for the scalar fields  $-\tilde{f} : R_f \rightarrow \mathbb{R}$  and  $-\tilde{g} : R_g \rightarrow \mathbb{R}$ , which proves the second half of Theorem 4.2. (Recall that while  $Dg_0(R_f)$  captures (minimum, down-fork) persistence pairs,  $Dg_0(R_g)$  captures (up-fork, maximum) persistence pairs.)  $\square$

## 4.2 Relation to Extended Persistence Diagram

Recall that the range of cycle features in the Reeb graph correspond to points in the 1st extended persistence diagram. In what follows we will show the following main theorem, which states that  $d_{FD}(R_f, R_g)$  is bounded below by the bottleneck distance between the 1st extended persistence diagrams  $ExDg_1(R_f)$  and  $ExDg_1(R_g)$ .

**THEOREM 4.3.**  $d_B(ExDg_1(R_f), ExDg_1(R_g)) \leq 3d_{FD}(R_f, R_g)$ .

For simplicity of exposition, we assume that  $d_{FD}(R_f, R_g)$  can be achieved by optimal continuous maps  $\phi : R_f \rightarrow R_g$  and  $\psi : R_g \rightarrow R_f$ . The case where  $d_{FD}(R_f, R_g)$  is achieved in the limit can be handled by considering a sequence of continuous maps that are optimal up to an arbitrarily small additive term  $\epsilon$ . Let  $\delta = d_{FD}(R_f, R_g)$ .

**Thin bases.** Let  $Z_1(R_f)$  be the 1-dimensional cellular cycle group of  $R_f$  with coefficients in  $\mathbb{Z}_2$ , i.e., the subgroup of the 1-dimensional cellular chains with zero boundary. Since the Reeb graph has the structure of a 1-dimensional CW complex, the 1-dimensional cellular boundary group is trivial, and so every *cellular* 1-cycle of  $R_f$  represents a unique homology class<sup>2</sup> in  $H_1(R_f)$ ; that is,  $H_1(R_f) \cong Z_1(R_f)$ .

For a cellular 1-cycle  $\gamma = \sum_a e_a$ , let  $\text{im } \gamma$  denote the union of the images of the characteristic maps for all 1-cells (edges)  $e_a$ . Let  $\text{range}(\gamma) = [\min_{x \in \text{im } \gamma} f(x), \max_{x \in \text{im } \gamma} f(x)]$  denote the *range* of a cycle  $\gamma$ , and let  $\text{height}(\gamma)$  be the length of this interval. A cycle is *thinner* than another one if its height is strictly smaller. A cycle  $\gamma$  is *thin* if it cannot be written as a linear combination of thinner cycles. See Fig. 1 (b), where the cycle  $x_4x_8x_6x_5x_9x_4$  is thin, while the cycle  $x_3x_4x_9x_5x_6x_3$  is not. Given a basis of  $Z_1(R_f)$ , consider the sequence of the heights of the cycles contained in it, ordered in non-decreasing order. A basis for  $Z_1(R_f)$  is a *thin* basis if its height

<sup>2</sup>Note that the same is not true for singular homology; this is the reason why we consider cellular cycles here.

sequence is less than or equal to that of any other basis of  $Z_1(R_f)$  in the lexicographic order.

From now on, we fix an arbitrary thin basis  $\mathcal{G}_f = \{\gamma_1, \dots, \gamma_n\}$  of  $Z_1(R_f)$  and  $\mathcal{G}_g = \{\zeta_1, \dots, \zeta_m\}$  of  $Z_1(R_g)$ , with  $n$  and  $m$  being the rank of  $Z_1(R_f)$  and  $Z_1(R_g)$ , respectively. It is known [14] that every cycle in a thin basis of  $R_f$  is necessarily a thin cycle, and the ranges  $[b, d]$  of cycles in  $\mathcal{G}_f$  (resp. in  $\mathcal{G}_g$ ) correspond one-to-one to the points  $(b, d)$  in the 1st extended persistence diagram  $ExDg_1(R_f)$  (resp. in  $ExDg_1(R_g)$ ). For example, in Fig. 1 (b), the two cycles  $x_3x_4x_8x_6x_3$  and  $x_4x_8x_6x_5x_9x_4$  form a thin basis, corresponding to points  $(\tilde{f}(x_8), \tilde{f}(x_3))$  and  $(\tilde{f}(x_9), \tilde{f}(x_4))$  in  $ExDg_1(R_f)$  in (d).

Given any cycle  $\gamma$  of  $R_f$  (resp. of  $R_g$ ), we can represent  $\gamma$  uniquely as a linear combination of cycles in  $\mathcal{G}_f$  (resp.  $\mathcal{G}_g$ ), which we call the *thin basis decomposition* of  $\gamma$ ; we omit the reference to  $\mathcal{G}_f$  and  $\mathcal{G}_g$  since they will be fixed from now on. The thin cycle with the largest height from the thin basis decomposition of  $\gamma$  is called the *dominating cycle* of  $\gamma$ , denoted by  $\text{dom}(\gamma)$ . If there are multiple cycles with the same maximal height, then by convention we choose the one with smallest index in  $\mathcal{G}_f$  (resp. in  $\mathcal{G}_g$ ) as the dominating cycle. A cycle  $\gamma$  is  $\alpha$ -stable if its dominating cycle has a height strictly larger than  $2\alpha$ . Let  $Z_1^\alpha(R_f)$  denote the subgroup of  $Z_1(R_f)$  generated by cycles with height at most  $2\alpha$ . Equivalently, a thin basis decomposition of a cycle in  $Z_1^\alpha(R_f)$  consists only of cycles with height at most  $2\alpha$ . Hence, a cycle  $z$  is in  $Z_1^\alpha(R_f)$  if and only if  $z$  is *not*  $\alpha$ -stable. Note that this only means that the *dominating* cycle of  $z$  has height at most  $2\alpha$ ; the height of  $z$  itself can be larger than  $2\alpha$ . We have the following property of the dominating cycle:

**LEMMA 4.4.** *A set of cycles  $\gamma_1, \dots, \gamma_k \in Z_1(R_f)$  with distinct dominating cycles is linearly independent.*

**PROOF.** We show that  $\sum_{j=1}^k \gamma_{i_j} \neq 0$  for any subset  $\{i_1, \dots, i_a\} \subseteq \{1, 2, \dots, k\}$ . Specifically, consider the maximum height of dominating cycles of any cycle in  $\{\gamma_{i_j}\}_{j=1}^a$ . First, assume that there is only a unique cycle, say  $\gamma_{i_a}$ , whose dominating cycle  $\text{dom}(\gamma_{i_a})$  has this maximum height. It then follows that this thin cycle  $\text{dom}(\gamma_{i_a})$  is not in the thin basis decomposition of any other cycle  $\gamma_{i_j}, j \neq a$ . Since the thin basis decomposition of the cycle  $\sum_{j=1}^a \gamma_{i_j}$  is simply the sum (modulo 2) of thin basis decomposition of each  $\gamma_{i_j}$ ,  $\text{dom}(\gamma_{i_a})$  must exist in the thin basis decomposition of the cycle  $\sum_{j=1}^a \gamma_{i_j}$ ; in fact,  $\text{dom}(\sum_{j=1}^a \gamma_{i_j}) = \text{dom}(\gamma_{i_a})$ . Therefore  $\sum_{j=1}^a \gamma_{i_j} \neq 0$ .

If there are multiple cycles whose dominating cycle has the maximal height, then we consider the one whose dominating cycle has the smallest index among all of them. The same argument as above shows that this cycle will present in the thin basis decomposition of the cycle  $\sum_{j=1}^a \gamma_{i_j}$ , implying that  $\sum_{j=1}^a \gamma_{i_j} \neq 0$ .  $\square$

**$\alpha$ -matching.** The main use of thin cycles is that we will prove Theorem 4.3 by showing the existence of an  $\alpha$ -matching between  $\mathcal{G}_f$  and  $\mathcal{G}_g$ . Specifically, two thin cycles  $\gamma_1$  and  $\gamma_2$  are  $\alpha$ -close if their ranges  $[a, b]$  and  $[c, d]$  are within Hausdorff distance  $\alpha$ , i.e.,  $|c - a| \leq \alpha$  and  $|d - b| \leq \alpha$ . (Note that two  $\alpha$ -close cycles can differ in height by at most  $2\alpha$ .) An  $\alpha$ -matching for  $\mathcal{G}_f$  and  $\mathcal{G}_g$  is a set of pairs  $\mathcal{M} \subset \mathcal{G}_f \times \mathcal{G}_g$  such that:

- (I) For each pair  $\langle \gamma, \zeta \rangle \in \mathcal{M}$ ,  $\gamma$  and  $\zeta$  are  $\alpha$ -close; and
- (II) Every  $\alpha$ -stable cycle in  $\mathcal{G}_f$  and  $\mathcal{G}_g$  (i.e., with height larger than  $2\alpha$ ) appears in exactly one pair of  $\mathcal{M}$ ; every other cycle appears in at most one pair.

Since each point  $(b, d)$  in the extended persistence diagram corresponds to the range  $[b, d]$  of a unique cycle in a given thin basis,  $d_B(ExDg_1(R_f), ExDg_1(R_g)) \leq \alpha$  if and only if there is an  $\alpha$ -matching

for  $\mathcal{G}_f$  and  $\mathcal{G}_g$ . Our goal now is to prove that there exists a  $3\delta$ -matching for  $\mathcal{G}_f$  and  $\mathcal{G}_g$ , which will then imply Theorem 4.3.

**Properties of  $\phi$  and  $\psi$ .** Recall that  $\phi : R_f \rightarrow R_g$  and  $\psi : R_g \rightarrow R_f$  are the optimal continuous maps that achieve  $\delta = d_{FD}(R_f, R_g)$ . We now investigate the effect of these maps on thin cycles. Note that  $\phi$  and  $\psi$  induce maps  $Z_1(R_f) \rightarrow Z_1(R_g)$  and  $Z_1(R_g) \rightarrow Z_1(R_f)$ . To simplify notation, we denote these maps by  $\phi$  and  $\psi$  as well. Lemma 4.5 below states that  $\psi$  is “close” to being an inverse of  $\phi$ . Lemmas 4.6 and 4.7 relate the range of  $\phi(\gamma)$  with the range of  $\gamma$ .

**LEMMA 4.5.** *Given any cycle  $\gamma \in Z_1(R_f)$ , we have  $\psi \circ \phi(\gamma) \in \gamma + Z_1^{2\delta}(R_f)$ . That is,  $\psi \circ \phi(\gamma) = \gamma + \gamma'$ , where  $\gamma'$  is not  $2\delta$ -stable. A symmetric statement holds for any cycle in  $R_g$ .*

**PROOF.** The input Reeb graph  $R_f$  is a finite graph, and there are only a finite number of (cellular) cycles. Hence there are only a finite number of height values (reals) that these cycles can have. Let  $\alpha$  denote the lowest height of any cycle whose height is strictly larger than  $4\delta$ . We set  $\rho$  to be any positive constant between 0 and  $\alpha - 4\delta$ ; that is,  $4\delta + \rho < \alpha$ . Note that if a cycle  $\gamma$  satisfies  $\text{height}(\gamma) \leq 4\delta + \rho < \alpha$ , then it is necessary that  $\text{height}(\gamma) \leq 4\delta$ .

Assume that  $\text{im } \gamma$  has only a single connected component – the case with multiple components can be handled in a component-wise manner. This means that  $\gamma$  is generated by a loop  $\ell$ , i.e., a closed curve on  $R_f$ , in the sense that we can consider  $\ell$  as a singular cycle and then use the isomorphism of singular homology and cellular cycles. Without loss of generality, we may assume that  $\ell$  is embedded; otherwise,  $\ell$  can be split into embedded subloops, which again can be treated separately. Now for the given loop  $\ell$ , let  $\tilde{\ell}$  denote  $\psi \circ \phi(\ell)$ , and for any point  $x$  on  $\ell$ , let  $\tilde{x} \in \tilde{\ell}$  denote  $\tilde{x} := \psi \circ \phi(x)$ . Since both  $(x, \phi(x))$  and  $(\tilde{x}, \phi(x))$  are in  $G(\phi, \psi)$ , by Eq. (5), there is an embedded path  $\pi(x, \tilde{x})$  connecting  $x$  to  $\tilde{x}$  with  $\text{range}(\pi(x, \tilde{x})) = [a, b]$ , where  $b - a \leq 2\delta$ .

Let  $\ell[x, x']$  and  $-\ell[x, x']$  denote the orientation-preserving and orientation-reversing subcurves of  $\ell$  from  $x$  to  $x'$ , respectively. Start with an arbitrary point  $x = x_0$  on  $\ell$ , and consider  $\tilde{x}_0$  on  $\tilde{\ell}$ . Since  $\psi \circ \phi$  is a continuous map, as we move  $x$  along  $\ell$  continuously,  $\tilde{x}$  moves continuously. In step  $i$ , as we move along  $\ell$  (starting from  $x_i$ ), we set  $x_{i+1}$  to be the first point such that the height of the loop  $\ell_i = \ell[x_i, x_{i+1}] \circ \pi(x_{i+1}, \tilde{x}_i) \circ -\ell[\tilde{x}_{i+1}, \tilde{x}_i] \circ \pi(\tilde{x}_i, x_i)$  is  $4\delta + \rho$ . If no such  $\ell_i$  exists before  $\tilde{x}$  moves back to  $\tilde{x}_0$ , then we set  $x_{i+1}$  to be  $x_0$ , and the process terminates. Since both  $\pi(x_{i+1}, \tilde{x}_{i+1})$  and  $\pi(\tilde{x}_i, x_i)$  are paths of height at most  $2\delta$ , the sum of the heights of  $\ell[x_i, x_{i+1}]$  and  $-\ell[\tilde{x}_i, \tilde{x}_{i+1}]$  must be at least  $\rho$ . Hence, for a fixed value  $\rho$ , this process terminates in a finite number of steps. Now let  $c_i$  denote the cellular cycle homologous to the loop  $\ell_i$  in the above construction. By construction, we have that  $\gamma = \tilde{\gamma} + \sum_i c_i$ , where  $\tilde{\gamma} = \psi \circ \phi(\gamma)$ . Since each  $c_i$  satisfies  $\text{height}(c_i) \leq \text{height}(\ell_i) \leq 4\delta + \rho < \alpha$ , as discussed earlier it then follows that  $\text{height}(c_i) \leq 4\delta$ . Hence  $c_i \in Z_1^{2\delta}(R_f)$  for each  $i$  and  $\gamma' = \sum_i c_i \in Z_1^{2\delta}(R_f)$ , implying that  $\psi \circ \phi(\gamma) = \tilde{\gamma} = \gamma + \gamma' \in \gamma + Z_1^{2\delta}(R_f)$ .  $\square$

**LEMMA 4.6.** *Given any thin cycle  $\gamma \in Z_1(R_f)$  with range  $[b, d]$ , we have that the range of any cycle in the thin basis decomposition of  $\phi(\gamma)$  must be contained in the interval  $[b - \delta, d + \delta]$ .*

**PROOF.** First, by Eq. (5), we have  $\max_{x \in R_f} |f(x) - g(\phi(x))| \leq \delta$ . Hence  $\text{range}(\phi(\gamma)) \subseteq [b - \delta, d + \delta]$ . Now let  $b'$  be the smallest left endpoint of the range of any cycle in the thin basis decomposition of  $\phi(\gamma)$ . We will prove that  $b' \geq b - \delta$ .

Suppose this is not case and  $b' < b - \delta$ . Now let  $\zeta_1, \dots, \zeta_a \in \mathcal{G}_g$ ,  $a \geq 1$ , denote all those cycles in the thin basis decomposition of  $\phi(\gamma)$  whose ranges have  $b'$  as the left endpoint. Set  $\rho = \zeta_1 + \dots + \zeta_a$ . Assume  $\zeta_a$  has the largest height among these thin cycles. Note that

$\text{range}(\zeta_{i_j}) \subseteq \text{range}(\zeta_{i_a})$  for any  $j < a$ , as all these ranges share the same left endpoint  $b'$ . Clearly  $\text{range}(\rho) \subseteq \text{range}(\zeta_{i_a})$ . On the other hand, by definition of  $b'$  and  $\zeta_{i_j}$ , all other cycles in the thin basis decomposition of  $\phi(\gamma)$  have a range whose left endpoint is strictly greater than  $b'$ . Let  $\rho'$  be the sum of these other cycles; we have that  $\phi(\gamma) = \rho + \rho'$ . Since the left endpoint of  $\text{range}(\rho')$  is strictly bigger than  $b'$ , the left endpoint of  $\text{range}(\rho)$  also has to be strictly bigger than  $b'$ , as otherwise the left endpoint of  $\text{range}(\rho + \rho')$  would be  $b'$ , which contradicts to the fact that the left endpoint of  $\text{range}(\phi(\gamma))$  is at least  $b - \delta > b'$ . In other words, it is necessary that  $\text{range}(\rho)$  is a proper subset of  $\text{range}(\zeta_{i_a})$ ; i.e.,  $\text{range}(\rho) \subset \text{range}(\zeta_{i_a})$ . This implies that  $\rho$  has strictly smaller height than  $\zeta_{i_a}$ . This however contradicts that  $\mathcal{G}_g$  is a thin basis, because we can replace  $\zeta_{i_a}$  in  $\mathcal{G}_g$  with  $\rho$  and obtain a basis element with smaller height (the resulting set of cycles remain independent). Therefore it is not possible that  $b' < b - \delta$ .

A symmetric argument shows that the largest right endpoint of the range of any cycle in the thin basis decomposition of  $\phi(\gamma)$  is at most  $d + \delta$ . Hence the range of any cycle in the thin basis decomposition of  $\phi(\gamma)$  is a subset of  $[b - \delta, d + \delta]$ .  $\square$

**LEMMA 4.7.** *For any  $2\delta$ -stable cycle  $\gamma \in Z_1(R_f)$ , we have*

$$\text{height}(\text{dom}(\phi(\gamma))) \geq \text{height}(\text{dom}(\gamma)) - 2\delta.$$

*A symmetric statement holds for any cycle of  $R_g$ .*

**PROOF.** Note that in this lemma,  $\gamma$  is not necessarily a thin loop. Let  $\gamma_s = \text{dom}(\gamma)$ ; since  $\gamma$  is  $2\delta$ -stable, we have  $\text{height}(\gamma_s) > 4\delta$ . First, we claim that  $\text{dom}(\psi \circ \phi(\gamma)) = \gamma_s$ . This is because by Lemma 4.5,  $\psi \circ \phi(\gamma) \in \gamma + Z_1^{2\delta}(R_f)$ . Since  $\text{height}(\gamma_s) > 4\delta$ ,  $\gamma_s$  still belongs to the thin basis decomposition of  $\psi \circ \phi(\gamma)$  and still has the largest height.

Now set  $\tilde{\gamma} = \phi(\gamma)$  with  $\zeta_{i_1} + \dots + \zeta_{i_a}$  being its thin basis decomposition. Observe that for any cycle  $\gamma'$  in  $R_f$ , we have that  $\text{height}(\phi(\gamma')) \leq \text{height}(\gamma') + 2\delta$ , which follows from the fact that for any  $x \in R_f$ ,  $|f(x) - g(\phi(x))| \leq \delta$ ; recall Eq. (5). A symmetric statement holds for a loop from  $R_g$ . We thus have:

$$\begin{aligned} \text{height}(\text{dom}(\psi(\tilde{\gamma}))) &= \text{height}(\text{dom}(\sum_{j=1}^a \psi(\zeta_{i_j}))) \leq \max_{j=1}^a \text{height}(\psi(\zeta_{i_j})) \\ &\leq \max_{j=1}^a [\text{height}(\zeta_{i_j}) + 2\delta] = \max_{j=1}^a \text{height}(\zeta_{i_j}) + 2\delta \\ &= \text{height}(\text{dom}(\tilde{\gamma})) + 2\delta. \end{aligned} \quad (6)$$

Since we have shown earlier that  $\text{dom}(\psi \circ \phi(\gamma)) = \gamma_s$ , it follows that  $\text{dom}(\psi(\tilde{\gamma})) = \text{dom}(\psi \circ \phi(\gamma)) = \gamma_s = \text{dom}(\gamma)$ . Combining this with Eq. (6), we have

$$\begin{aligned} \text{height}(\text{dom}(\phi(\gamma))) &= \text{height}(\text{dom}(\tilde{\gamma})) \geq \text{height}(\text{dom}(\psi(\tilde{\gamma}))) - 2\delta \\ &= \text{height}(\text{dom}(\gamma)) - 2\delta, \end{aligned}$$

which proves the lemma.  $\square$

In fact, if  $\gamma$  is a thin cycle, Lemma 4.7 can be strengthened to show that  $\text{dom}(\phi(\gamma))$  is  $\delta$ -close to  $\gamma$ . This already provides some mapping of base cycles from  $\mathcal{G}_f$  to cycles from  $\mathcal{G}_g$  such that each pair of corresponding cycles are  $\delta$ -close. However, the main challenge is to show that there exists a *one-to-one* correspondence for all  $3\delta$ -stable cycles (recall the definition of a  $3\delta$ -matching of  $\mathcal{G}_f$  and  $\mathcal{G}_g$ ). For this, we need to take a slight detour to relate cycles in  $\mathcal{G}_f$  with those in  $\mathcal{G}_g$  in a stronger sense:

**PROPOSITION 4.8.** *For any thin cycle  $\gamma_k \in \mathcal{G}_f$ , one can compute a (not necessarily thin) cycle  $\widehat{\gamma}_k$  such that  $\gamma_k = \text{dom}(\widehat{\gamma}_k)$  and*

$$\phi(\widehat{\gamma}_k) \in \sum_{j=1}^r \zeta_{k_j} + Z_1^{2\delta}(R_g),$$

where each  $\zeta_{kj} \in \mathcal{G}_g$  is  $3\delta$ -close to  $\gamma_k$ , for any  $j \in [1, r]$ .

PROOF. Assume that the thin basis decomposition of  $\phi(\gamma_k)$  has the form:

$$\phi(\gamma_k) \in \sum_{j=1}^r \zeta_{kj} + \sum_{j=1}^s \tilde{\zeta}_j + Z_1^{2\delta}(R_g),$$

where the first term contains the  $2\delta$ -stable thin cycles whose range is  $3\delta$ -Hausdorff close to  $\text{range}(\gamma_k)$ , the last term contains the thin cycles that are not  $2\delta$ -stable, and the middle term contains those thin cycles  $\tilde{\zeta}_j$  that are neither  $3\delta$ -close to  $\gamma_k$  nor small. We wish to get rid of the middle term  $\tilde{\zeta} = \sum_{j=1}^s \tilde{\zeta}_j$ . Set  $\gamma' = \psi(\tilde{\zeta})$ . By Lemma 4.5, we have that  $\phi(\gamma') = \phi \circ \psi(\tilde{\zeta}) \in \tilde{\zeta} + Z_1^{2\delta}(R_g)$ . Set  $\widehat{\gamma}_k := \gamma_k + \gamma'$ . It is then easy to verify that  $\phi(\widehat{\gamma}_k) = \phi(\gamma_k) + \phi(\gamma') \in \sum_{j=1}^r \zeta_{kj} + Z_1^{2\delta}(R_g)$ , as claimed.

It remains to show that  $\text{dom}(\widehat{\gamma}_k) = \gamma_k$ . Let  $[b, d] = \text{range}(\gamma_k)$ . By Lemma 4.6,  $\text{range}(\tilde{\zeta}_j) \subseteq [b - \delta, d + \delta]$ , for any  $j \in [1, s]$ . Since each  $\tilde{\zeta}_j$  is not  $3\delta$ -close to  $\gamma_k$ , it is then necessary that, for any  $j \in [1, s]$ , either  $\text{range}(\tilde{\zeta}_j) \subseteq [b - \delta, d - 3\delta]$  or  $\text{range}(\tilde{\zeta}_j) \subseteq (b + 3\delta, d + \delta]$ . W.l.o.g. assume that  $\text{range}(\tilde{\zeta}_j) \subseteq [b - \delta, d - 3\delta]$ . Apply Lemma 4.6 to the cycle  $\tilde{\zeta}_j$ . We have that the range of any cycle in the thin basis decomposition of  $\psi(\tilde{\zeta}_j)$  is contained in  $[b - 2\delta, d - 2\delta]$ , thus its height strictly smaller than  $d - b$ . Hence all cycles in the thin basis decomposition of  $\gamma' = \psi(\tilde{\zeta})$  have a height strictly smaller than  $\text{height}(\gamma_k) = d - b$ . This means that  $\gamma_k$  has the largest height among the cycles of the thin basis decomposition of  $\widehat{\gamma}_k = \gamma_k + \gamma'$ , and it is the only cycles with this largest height. It then follows that  $\gamma_k = \text{dom}(\widehat{\gamma}_k)$ .  $\square$

COROLLARY 4.9. Let  $\widehat{\mathcal{G}}_f$  denote the set of cycles  $\{\widehat{\gamma}_k\}_{k=1}^n$ , where each  $\widehat{\gamma}_k$  is as specified in Proposition 4.8.  $\widehat{\mathcal{G}}_f$  forms a basis for  $Z_1(R_f)$ .

PROOF. Since the dominating cycles for cycles in  $\widehat{\mathcal{G}}_f$  are all distinct, it follows from Lemma 4.4 that all cycles in  $\widehat{\mathcal{G}}_f$  are linearly independent. Hence  $\widehat{\mathcal{G}}_f$  also forms a (not necessarily thin) basis for  $Z_1(R_f)$ .  $\square$

Let  $\Phi$  denote the matrix of the mapping from the base cycles in  $\widehat{\mathcal{G}}_f$  (columns, domain) to those in  $\mathcal{G}_g$  (rows, range) as induced by  $\phi$ , i.e., the  $i$ th column of  $\Phi$  specifies the representation of  $\phi(\widehat{\gamma}_i)$  using basis elements from  $\mathcal{G}_g$ , with  $\Phi_{ij} = 1$  if  $\zeta_j$  is in the thin basis decomposition of  $\phi(\widehat{\gamma}_i)$ . Let  $\widetilde{\Phi}$  be the submatrix of  $\Phi$  with columns corresponding to basis elements  $\widehat{\gamma}_i$  that are  $3\delta$ -stable, and rows corresponding to basis elements  $\zeta_j$  that are  $2\delta$ -stable. See Fig. 2 (a). By Proposition 4.8,  $\widetilde{\Phi}_{ij} = 1$  implies that the basis element  $\zeta_j \in \mathcal{G}_g$  is  $3\delta$ -close to the basis element  $\gamma_i \in \mathcal{G}_f$ . Recall that our goal is to show that there is a  $3\delta$ -matching for  $\mathcal{G}_f$  and  $\mathcal{G}_g$ . Intuitively, non-zero entries in  $\widetilde{\Phi}$  will provide potential matchings for basis elements in  $\mathcal{G}_f$  to establish a  $3\delta$ -matching between  $\mathcal{G}_f$  and  $\mathcal{G}_g$  that we need.

LEMMA 4.10. The columns of  $\widetilde{\Phi}$  are linearly independent.

PROOF. Consider an arbitrary subset of indices  $i_1, \dots, i_s$  whose corresponding columns are in  $\widetilde{\Phi}$  (i.e., each  $\widehat{\gamma}_{i_a}$  is  $3\delta$ -stable), and let  $\widehat{\gamma} = \widehat{\gamma}_{i_1} + \dots + \widehat{\gamma}_{i_s}$ . We will show that  $\phi(\widehat{\gamma})$  is  $2\delta$ -stable; that is,  $\text{dom}(\phi(\widehat{\gamma}))$  has height at least  $4\delta$ . This means that the linear combination of the corresponding columns in  $\widetilde{\Phi}$  contains a non-zero element. Since this holds for any subset of columns from  $\widetilde{\Phi}$ , we have that the columns in  $\widetilde{\Phi}$  are linearly independent.

It remains to show that  $\phi(\widehat{\gamma})$  is  $2\delta$ -stable. Recall that for any index  $a$ ,  $\gamma_a$  is the dominating cycle of  $\widehat{\gamma}_a$ . Assume w.l.o.g. that  $\gamma_{i_1}$  has the largest height among all  $\gamma_{i_j}$ , for  $j \in [1, s]$ . (If there are multiple

cycles from  $\{\gamma_{i_j}\}_{j=1}^s$  having this largest height, let  $\gamma_{i_1}$  be the one with smallest index.) From the end of the proof of Proposition 4.8, we note that for any index  $a$ ,  $\gamma_a$  is the *only* cycle with maximum height among all cycles in the thin basis decomposition of  $\widehat{\gamma}_a$ . In other words, all other cycles in the thin basis decomposition of  $\widehat{\gamma}_a$  have strictly smaller height than  $\gamma_a$ . Putting these together, it follows that  $\gamma_{i_1}$  must exist in the thin basis decomposition of  $\widehat{\gamma}$  w.r.t. the original thinnest basis  $\mathcal{G}_f$  and in fact,  $\gamma_{i_1} = \text{dom}(\widehat{\gamma})$ . Since  $\gamma_{i_1}$  is  $3\delta$ -stable (thus its height at least  $6\delta$ ), it then follows from Lemma 4.7 that  $\text{height}(\text{dom}(\phi(\widehat{\gamma}))) \geq \text{height}(\text{dom}(\widehat{\gamma})) - 2\delta > 4\delta$ . So  $\phi(\widehat{\gamma})$  is  $2\delta$ -stable.  $\square$

COROLLARY 4.11. We can identify a unique row index  $i$  for each column index  $j$  in  $\widetilde{\Phi}$  such that  $\Phi_{ij} = 1$ .

PROOF. View the matrix  $\widetilde{\Phi}$  as the adjacency matrix for the following bipartite graph  $G = (P \cup Q, E)$ , where  $P$  are the columns of  $\widetilde{\Phi}$ ,  $Q$  are the rows, and there is an edge between  $p \in P$  and  $q \in Q$  iff the corresponding entry in the matrix  $\widetilde{\Phi}$  is 1. We now claim that there is a  $P$ -saturated matching for  $G$ : that is, there is a matching of  $G$  such that every node in  $P$  is matched exactly once, and each node in  $Q$  is matched at most once. Note that this immediately implies the claim. Specifically, for any subset of nodes  $P' \subseteq P$ , let  $Q' \subseteq Q$  be the union of neighbors of nodes from  $P'$ . In other words,  $Q'$  is the set of rows with at least one non-zero entry in the columns  $P'$ . If  $|Q'| < |P'|$ , then these columns of  $\widetilde{\Phi}$  will be linearly dependent, which violates Lemma 4.10. Hence we have  $|Q'| \geq |P'|$ . Now by Hall's Theorem (see, e.g., Page 35 of [34]), a  $P$ -saturated matching exists for  $G$ .  $\square$

**Proof of Theorem 4.3.** Recall that by Proposition 4.8,  $\widetilde{\Phi}_{ij} = 1$  implies that the cycles  $\gamma_j$  and  $\zeta_i$  are  $3\delta$ -close. It follows from Corollary 4.11 that there is an injective map  $F$  from the set of  $3\delta$ -stable cycles in  $\mathcal{G}_f$  to the cycles in  $\mathcal{G}_g$  such that each pair of corresponding cycles are  $3\delta$ -close. By a symmetric argument (switching the role of  $R_f$  and  $R_g$ ), there is also an injective map  $G$  from the  $3\delta$ -stable cycles in  $\mathcal{G}_g$  to cycles in  $\mathcal{G}_f$  where each corresponding pair of cycles are  $3\delta$ -close. However,  $F$  and  $G$  may not be consistent and do not directly give rise to a  $3\delta$ -matching of  $\mathcal{G}_f$  and  $\mathcal{G}_g$  yet. In what follows, we will modify  $F$  to obtain another *injective* map  $\widehat{F}$  such that (i) any  $3\delta$ -stable cycle in  $\mathcal{G}_f$  is mapped by  $\widehat{F}$  to a cycle in  $\mathcal{G}_g$  that is  $3\delta$ -close, and (ii) all  $3\delta$ -stable cycles in  $\mathcal{G}_g$  are contained in  $\text{im } \widehat{F}$ , the image of  $\widehat{F}$ . Note that  $\widehat{F}$  provides exactly the set of correspondences necessary in a  $3\delta$ -matching between  $\mathcal{G}_f$  and  $\mathcal{G}_g$ . In particular, the injectivity of  $\widehat{F}$  and these conditions guarantee that the condition (II) of a  $3\delta$ -matching. As discussed at the beginning of this section, this then means that  $d_B(\text{ExDg}_1(R_f), \text{ExDg}_1(R_g)) \leq 3\delta = 3d_{FD}(R_f, R_g)$ , proving Theorem 4.3.

It remains to show how to construct  $\widehat{F}$  satisfying conditions (i) and (ii) above. Conditions (i) already holds for  $F$ , so the main task is to establish condition (ii) while maintaining (i). Start with  $\widehat{F} = F$ . Let  $y_0 \notin \text{im } \widehat{F}$  be any  $3\delta$ -stable cycle in  $\mathcal{G}_g$  that is not yet in  $\text{im } \widehat{F}$ . Let  $x_1 = G(y_0) \in \mathcal{G}_f$ . We continue with  $y_i = \widehat{F}(x_i)$  if  $x_i$  is  $3\delta$ -stable. Next, if  $y_i$  is  $3\delta$ -stable, then set  $x_{i+1} = G(y_i)$ . We repeat this process, until we reach  $x_k$  or  $y_k$  which is not  $3\delta$ -stable any more. At this time, we modify  $\widehat{F}(x_i)$  to be  $y_{i-1}$  for each  $j \in [1, k]$  (originally,  $\widehat{F}(x_i) = y_i$ ). Throughout this process, all  $y_i$  other than  $y_0$  are already in  $\text{im } \widehat{F}$ . After the modification of  $\widehat{F}$ , we have  $y_0 \in \text{im } \widehat{F}$ , while all other  $y_i$  remain in  $\text{im } \widehat{F}$ . The only exception is when the above process terminates by reaching some  $y_k$  which is not  $3\delta$ -stable (the termination condition), in which case  $y_k$  will not be in  $\text{im } \widehat{F}$  after the modification of  $\widehat{F}$ . However, the number of  $3\delta$ -stable

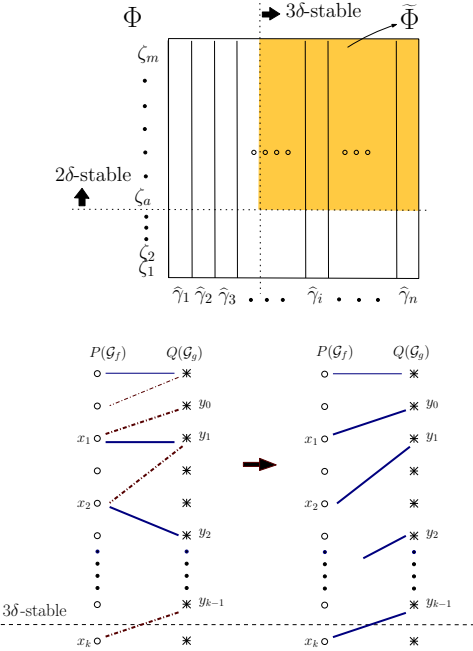


**Figure 2:** Top: The  $i$ th column in the matrix  $\Phi$  specifies the representation of  $\phi(\tilde{\gamma}_i)$  using the basis elements in  $\mathcal{G}_g$ . The shaded submatrix represents  $\tilde{\Phi}$ . Bottom: A bipartite graph view of the augmenting process. Left: Thick path alternates between an  $F$ -induced (solid) and a  $G$ -induced (dash-dotted) edge. Right: Thick solid edges are induced by the modified injective map  $\tilde{F}$  (which are used to be  $G$ -induced edges in the left figure).

cycles contained in  $\text{im } \widehat{F}$  increases by one (i.e.,  $y_0$ ) by the above process. It is easy to verify that since  $F$  is injective,  $\widehat{F}$  remains injective. Furthermore,  $x_i$  and  $y_{i-1} = \widehat{F}(x_i)$  are still  $3\delta$ -close, since by construction  $x_i = G(y_{i-1})$ .

An alternative way to view this is to consider the specific bipartite graph  $G' = (P \cup Q, E')$ , where nodes in  $P$  and  $Q$  correspond to basis cycles in  $\mathcal{G}_f$  and  $\mathcal{G}_g$ , respectively, and edges  $E'$  are those corresponding to a cycle and its image under either the map  $\widehat{F}$  or  $G$ . The sequence  $y_0, x_1, y_1, \dots$  specifies a path with edges alternating between the  $\widehat{F}$ -induced and the  $G$ -induced matchings. The modified assignment of  $\widehat{F}(x_j)$  changes a  $G$ -induced matching to an  $\widehat{F}$ -induced matching along this path, much similar to the use of augmenting paths to obtain maximum bipartite matching. See Fig. 2 (b) for an illustration.

We repeat the above path augmentation process for any remaining  $3\delta$ -stable cycle in  $\mathcal{G}_g \setminus \text{im } \widehat{F}$ . This process will terminate because after each augmentation process, the number of  $3\delta$ -stable cycles contained in  $\text{im } \widehat{F}$  strictly increases. In the end, we obtain an injective map  $\widehat{F}$  from the set of  $3\delta$ -stable cycles of  $\mathcal{G}_f$  to cycles in  $\mathcal{G}_g$  such that  $\text{im } \widehat{F}$  contains all  $3\delta$ -stable cycles of  $\mathcal{G}_g$ . Hence,  $\widehat{F}$  induces a  $3\delta$ -matching from  $\text{ExDg}_1(R_f)$  to  $\text{ExDg}_1(R_g)$ , finishing the proof of Theorem 4.3.

### 4.3 Further Discussion

The proof of Theorem 4.2 leverages a beautiful stability result for a pair of interleaving persistence modules, originally introduced in [10] and recently generalized in [2, 12]. This approach however, is not immediately applicable to bound the relation to the extended persistence diagrams in our case (i.e, to prove Theorem 4.3), since the extended persistence module is not parametrized over the re-

als, but over two copies of the real line. Therefore, the notion of interleaving distance does not apply directly.

A better choice to capture the extended persistence diagrams seems to be the persistent homology of *interlevel sets* [7, 8, 16] (specifically, see the discussion on the relation to extended persistence diagrams in [8]). Unfortunately, it is not yet clear how to obtain a bound on the bottleneck distance from a given interleaving of the 0th homology groups of interlevel sets. In the case of ordinary persistence modules, an explicit matching of persistence diagrams induced by an interleaving is described in [2]. We plan to investigate the use of this construction in the context of Reeb graphs.

## 5. SIMPLIFICATION OF REEB GRAPHS

### 5.1 A Natural Simplification Strategy

Simplifying a Reeb graph can help to remove noise and to create multi-resolution representations of input scalar fields. As described in Section 2, there is a natural way to define the “importance” of branching and cycle features, which is equivalent to ordinary and extended persistence in according dimensions. It is common in practice to simplify the Reeb graph by removing all features with persistence smaller than a certain threshold  $\delta$ . We now introduce a natural simplification scheme for Reeb graphs (see, e.g., [20, 29]). See Fig. 3 for an illustration.

Given an ordinary persistence pair  $(m, s)$ , assume that  $m$  is a minimum and  $s$  is a down-fork. Recall that the down-fork  $s$  merges two connected components  $C_1$  and  $C_2$  of the sublevel set below  $f(s)$ , and  $m$  is the higher minimum of the two. To remove the feature  $(m, s)$ , we wish to merge the branch containing  $m$ , say  $C_1$ , into the other branch  $C_2$ , so that afterwards,  $m$  and  $s$  become regular points (i.e., with up-degree and down-degree both being 1). In particular, we perform the following operation (see Fig. 3 (a)). Let  $m_2$  denote the minimum of  $C_2$ . We choose an arbitrary embedded path  $\pi_1 \subseteq C_1$  from  $s$  to  $m$ , and an arbitrary path  $\pi' \subseteq C_2$  from  $s$  to  $m_2$ . Now imagine we traverse  $\pi'$  starting from  $s$ . We stop when we encounter the first point  $x$  on  $\pi'$  such that  $f(x) = f(m)$ , and set  $\pi_2$  to be the subcurve of  $\pi'$  from  $s$  to  $x$ . By identifying points with the same function value, we merge  $\text{im } \pi_1$  and  $\text{im } \pi_2$  to form the image of a new monotonic arc  $\pi_3$  between  $s$  and  $x$  such that any point  $p \in \text{im } \pi_1 \cup \text{im } \pi_2$  is mapped to some  $q \in \text{im } \pi_3$  with  $f(q) = f(p)$ . Pairs of type (up-fork, maximum) are treated in a symmetric way.

Given an extended persistence pair  $(s_1, s_2)$  between an up-fork  $s_1$  and a down-fork  $s_2$ , let  $\gamma$  be a thin cycle that spans it. W.l.o.g. assume that  $\text{im } \gamma$  consists only of a single connected component: if  $\text{im } \gamma$  has multiple connected components, then there must exist one that contains both  $s_1$  and  $s_2$ . That component is necessarily an embedded loop and thus we can simply set  $\gamma$  to be the thin cycle corresponding to that loop. Let  $\pi_1$  and  $\pi_2$  denote the two disjoint sub-curves of the loop that connect  $s_1$  and  $s_2$ . To cancel the feature, intuitively, we wish to merge  $\pi_1$  and  $\pi_2$  to kill the cycle  $\gamma$ . Note that  $\pi_1$  and  $\pi_2$  may not be monotonic (w.r.t. the input function  $f$ ); however, all points in  $\pi_1$  and  $\pi_2$  have function values within the range  $[f(s_1), f(s_2)]$ . The merging of  $\pi_1$  and  $\pi_2$  results in a new monotonic arc  $\pi_3$  from  $s_1$  and  $s_2$ , such that every point  $p \in \text{im } \gamma$  is mapped to some  $q \in \pi_3$  with  $f(q) = f(p)$ . See Fig. 3 (b) for an illustration.

Note that since a critical pair  $(m, s)$  (resp. an essential pair  $(s_1, s_2)$ ) corresponds uniquely to a persistence pair  $(f(m), f(s))$  in the ordinary persistence diagram (resp.  $(f(s_1), f(s_2))$  in the extended persistence diagram), the above process also removes a point from the respective persistence diagram.

Let  $R$  and  $R'$  denote the Reeb graph before and after the simplification of a persistence pair  $\tau = (b, d)$  by collapsing its corresponding

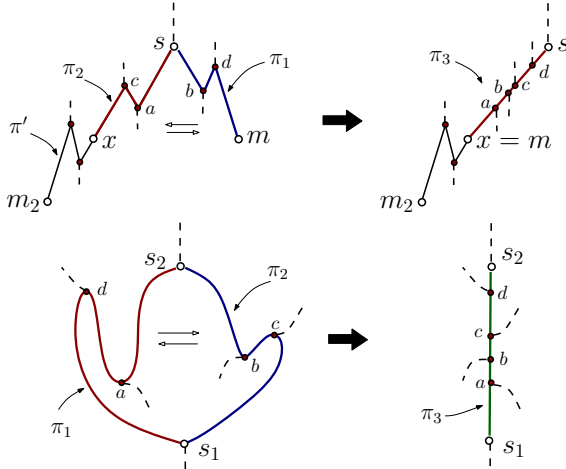


**Figure 3: Top:** Removing a branching feature spanned by  $(m, s)$  by merging paths  $\pi_1$  and  $\pi_2$ . This removes the point  $(f(m), f(s))$  from the 0-th ordinary persistence diagram. **Bottom:** Removing a cycle feature spanned by  $(s_1, s_2)$ ; this removes the point  $(f(s_1), f(s_2))$  from the 1st extended persistence diagram.

branching or loop feature. Let  $\pi_1^\tau$  and  $\pi_2^\tau$  be as introduced above. Call  $\gamma^\tau = \pi_1^\tau \cup \pi_2^\tau$  the *merging path* w.r.t.  $\tau$ . Note that  $\gamma^\tau$  is a closed curve corresponding to a thin cycle spanning  $(b, d)$  when it is an extended persistence pair, and a connected path with  $b$  and  $d$  being the respective minimum and maximum function values on it otherwise. The merging path  $\gamma^\tau$  will be collapsed into a single monotonic arc in order to eliminate the persistence pair  $\tau$ . We can view the removal of  $\tau$  in a more formal way as follows: We say that two points  $x, y \in R$  are  $\tau$ -equivalent, denoted by  $x \sim_\tau y$ , if  $f(x) = f(y)$  and  $x, y \in \gamma^\tau$ . The simplified Reeb graph  $R'$  is the quotient space  $R/\sim_\tau$ ; the corresponding quotient map  $\mu_\tau : R \rightarrow R'$  satisfies  $\mu_\tau(x) = \mu_\tau(y)$  if and only if  $x \sim_\tau y$ . The function  $f : R \rightarrow \mathbb{R}$  induces a function  $f' : R' \rightarrow \mathbb{R}$  such that for any  $x' \in R'$ ,  $f'(x') = f(x)$  for any  $x \in \mu_\tau^{-1}(x')$ .

Now given an input Reeb graph  $R$ , suppose we wish to eliminate a set of  $k$  persistence pairs  $\{\tau_1 = (b_1, d_1), \tau_2 = (b_2, d_2), \dots, \tau_k = (b_k, d_k)\}$ . Compute the merging path  $\gamma^{\tau_i}$  for each persistence pair  $\tau_i$  in  $R$ . We now define an equivalence relation  $\sim$  as the transitive closure of all  $\sim_{\tau_i}$ 's for  $i \in [1, k]$ . This is equivalent to collapsing  $\gamma^{\tau_i}$ 's for all  $i \in [1, k]$  in an arbitrary order to kill the persistence pairs  $\tau_1, \dots, \tau_k$ . The final simplified Reeb graph  $\tilde{R}$  is obtained as the quotient space  $R/\sim$ . We have a well-defined function  $g : \tilde{R} \rightarrow \mathbb{R}$  induced by the function  $f : R \rightarrow \mathbb{R}$  such that  $g(\mu(x)) = f(x)$  for any  $x \in R$ .

## 5.2 Distance Between a Reeb Graph and its Simplification

While the simplification scheme described in previous section removes a set of persistence pairs  $\tau_1, \dots, \tau_k$ , it is not immediately clear how other points in the persistence diagram of the original Reeb graph  $R$  are affected. To this end, we wish bound the bottleneck distance between the persistence diagrams of  $f : R \rightarrow \mathbb{R}$  and  $g : \tilde{R} \rightarrow \mathbb{R}$  (defined at the end of Section 5.1). Specifically, it turns out that we can have the following result on the functional distortion distance between  $R$  and its simplification  $\tilde{R}$ :

**LEMMA 5.1.** *Let  $\tilde{R}$  be the simplified Reeb graph as described in Section 5.1 by removing  $k$  persistence pairs  $\{\tau_1 = (b_1, d_1), \tau_2 =$*

*$(b_2, d_2), \dots, \tau_k = (b_k, d_k)\}$ . Let  $\delta$  denote the largest persistence of  $\tau_1, \dots, \tau_k$ . We then have that  $d_{FD}(R, \tilde{R}) \leq 2\delta$ .*

The above lemma is shown by constructing specific continuous maps  $\phi : R \rightarrow \tilde{R}$  and  $\psi : \tilde{R} \rightarrow R$ , and showing that each of the three terms in Eq. (5) is bounded from above by  $2\delta$ , which in turn provides an upper bound for  $d_{FD}(R, \tilde{R})$ . The details are omitted from this extended abstract and can be found in [3]. Combining Lemma 5.1 with Theorems 4.2 and 4.3, we conclude with the following main result on the simplification of the Reeb graphs:

**THEOREM 5.2.** *Suppose we simplify a Reeb graph  $R$  by removing features of persistence  $\leq \delta$  using the strategy detailed in Section 5.1. The bottleneck distance between the (ordinary and extended) persistence diagram for  $R$  and its simplification  $\tilde{R}$  is at most  $6\delta$ .*

## 6 CONCLUDING REMARKS

In this paper, we propose a distance for Reeb graphs, under which the Reeb graph is stable with respect to changes in the input function under the  $L_\infty$  norm. More importantly, we show that this distance is bounded from below by and thus more discriminative at differentiating scalar fields than the bottleneck distance between both 0th ordinary and 1st extended persistence diagrams. Similar to the use of the Gromov-Hausdorff distance for metric spaces, having the Reeb graph distance metric provides a formal language for describing and studying various properties of the Reeb graphs. Indeed, we have already shown that, by bounding the functional distortion distance between a Reeb graph and its simplification, we can prove that important (persistent) features are preserved under simplification, which addresses a key practical issue.

Our current bound in Theorem 4.3 has a constant factor of 3. It will be interesting to see whether this factor can be improved to 1 to match the bound in Theorem 4.2, either for the functional distortion distance or for some other distance.

A natural question is how to compute the functional distortion distance. We believe that there is an exponential time algorithm to approximate  $d_{FD}(R_f, R_g)$ , similar to what is known for the  $\varepsilon$ -interleaving distance for merge trees [26]. However, it remains an open problem to develop more efficient algorithms. We remark that comparing unlabeled trees is computationally hard in general: The commonly used tree edit distance and tree alignment distance are NP-hard to compute (and sometimes even to approximate) [6]. Similarly, no polynomial time algorithms yet exist for the Gromov-Hausdorff distance in general. It will be interesting to see whether by leveraging the scalar field associated with merge trees and Reeb graphs, more efficient exact or approximation algorithms for computing functional distortion distance can be developed.

## Acknowledgements

We thank Facundo Mémoli for helpful discussions about variants of the Gromov–Hausdorff distance, which lead to improvements in our definition of the functional distortion distance. This research is partially supported by the National Science Foundation under grants CCF-1319406, CCF-1116258, and by the Toposys project FP7-ICT-318493-STREP.

## References

- [1] P. K. Agarwal, H. Edelsbrunner, J. Harer, and Y. Wang. *Extreme elevation on a 2-Manifold*. *Discrete Comput. Geom.*, 36(4):553–572, 2006.
- [2] U. Bauer and M. Lesnick. *Induced matchings of barcodes and the algebraic stability of persistence*. In *Proc. 30th Annu. ACM Symp. Comput. Geom.*, 2014.

- [3] U. Bauer, X. Ge, and Y. Wang. [Measuring distance between Reeb graphs](#). Preprint, 2014. [arXiv:1307.2839](https://arxiv.org/abs/1307.2839).
- [4] K. Beketayev, D. Yeliussizov, D. Morozov, G. H. Weber, and B. Hamann. Measuring the distance between merge trees. In *TopoInVis'13*, 2013.
- [5] S. Biasotti, D. Giorgi, M. Spagnuolo, and B. Falcidieno. [Reeb graphs for shape analysis and applications](#). *Theor. Comput. Sci.*, 392(1-3):5–22, 2008.
- [6] P. Bille. [A survey on tree edit distance and related problems](#). *Theor. Comput. Sci.*, 337(1-3):217–239, 2005.
- [7] G. Carlsson and V. de Silva. [Zigzag persistence](#). *Foundations of Computational Mathematics*, 10(4):367–405, 2010.
- [8] G. Carlsson, V. de Silva, and D. Morozov. [Zigzag persistent homology and real-valued functions](#). In *Proc. 25th Annu. ACM Sympos. Comput. Geom.*, pages 247–256, 2009.
- [9] F. Chazal and J. Sun. [Gromov-Hausdorff approximation of filament structure using Reeb-type graph](#). In *Proc. 30th Annu. ACM Sympos. Comput. Geom., To appear*, 2014.
- [10] F. Chazal, D. Cohen-Steiner, M. Glisse, L. J. Guibas, and S. Oudot. [Proximity of persistence modules and their diagrams](#). In *Proc. 25th ACM Sympos. on Comput. Geom.*, pages 237–246, 2009.
- [11] F. Chazal, D. C. Steiner, L. J. Guibas, F. Mémoli, and S. Y. Oudot. [Gromov-Hausdorff stable signatures for shapes using persistence](#). In *Proceedings of the Symposium on Geometry Processing*, SGP '09, pages 1393–1403. Eurographics Association, 2009.
- [12] F. Chazal, V. de Silva, M. Glisse, and S. Oudot. [The structure and stability of persistence modules](#). Preprint, 2012. [arXiv:1207.3674](https://arxiv.org/abs/1207.3674).
- [13] D. Cohen-Steiner, H. Edelsbrunner, and J. Harer. [Stability of persistence diagrams](#). *Discrete Comput. Geom.*, 37(1):103–120, 2007.
- [14] D. Cohen-Steiner, H. Edelsbrunner, and J. Harer. [Extending persistence using Poincaré and Lefschetz duality](#). *Foundations of Computational Mathematics*, 9(1):79–103, 2008.
- [15] T. Dey and Y. Wang. [Reeb graphs: Approximation and persistence](#). *Discrete Comput. Geom.*, 49(1):46–73, 2013.
- [16] T. K. Dey and R. Wenger. [Stability of critical points with interval persistence](#). *Discrete Comput. Geom.*, 38(3):479–512, 2007.
- [17] B. Di Fabio and C. Landi. [Stability of Reeb graphs of closed curves](#). *Electronic Notes in Theoretical Computer Science*, 283:71–76, 2012.
- [18] H. Edelsbrunner and J. Harer. *Computational Topology: An Introduction*. Amer. Math. Soc., Providence, Rhode Island, 2009.
- [19] H. Edelsbrunner, D. Letscher, and A. Zomorodian. [Topological persistence and simplification](#). *Discrete Comput. Geom.*, 28(4):511–533, 2002.
- [20] X. Ge, I. Safa, M. Belkin, and Y. Wang. [Data skeletonization via Reeb graphs](#). In *Proc. 25th Annu. Conf. Neural Infor. Process. Sys. (NIPS)*, pages 837–845, 2011.
- [21] W. Harvey, R. Wenger, and Y. Wang. [A randomized  \$O\(m \log m\)\$  time algorithm for computing Reeb graph of arbitrary simplicial complexes](#). In *Proc. 25th Annu. ACM Sympos. Compu. Geom.*, pages 267–276, 2010.
- [22] A. Hatcher. *Algebraic Topology*. Cambridge University Press, 2002.
- [23] F. Hétroy and D. Attali. [Topological quadrangulations of closed triangulated surfaces using the Reeb graph](#). *Graph. Models*, 65(1-3):131–148, 2003.
- [24] M. Hilaga, Y. Shinagawa, T. Kohmura, and T. L. Kunii. [Topology matching for fully automatic similarity estimation of 3D shapes](#). In *Proc. SIGGRAPH '01*, pages 203–212, 2001.
- [25] N. J. Kalton and M. I. Ostrovskii. [Distances between Banach spaces](#). *Forum Mathematicum*, 11(1), 2008.
- [26] D. Morozov, K. Beketayev, and G. Weber. Interleaving distance between merge trees, 2013. Manuscript.
- [27] M. Natali, S. Biasotti, G. Patanè, and B. Falcidieno. [Graph-based representations of point clouds](#). *Graphical Models*, 73(5):151 – 164, 2011.
- [28] S. Parsa. [A deterministic  \$O\(m \log m\)\$  time algorithm for the Reeb graph](#). In *Discrete Comput. Geom.*, volume 49, pages 864–878. Springer-Verlag, 2013.
- [29] V. Pascucci, G. Scorzelli, P.-T. Bremer, and A. Mascarenhas. [Robust on-line computation of Reeb graphs: simplicity and speed](#). *ACM Trans. Graph. (SIGGRAPH 2007)*, 26(3), 2007.
- [30] G. Reeb. [Sur les points singuliers d'une forme de Pfaff complètement intégrable ou d'une fonction numérique](#). *Comptes Rendus Hebdomadaires des Séances de l'Académie des Sciences*, 222:847–849, 1946.
- [31] Y. Shinagawa, T. Kunii, and Y. L. Kergosien. [Surface coding based on Morse theory](#). *IEEE Comput. Graph. Appl.*, 11(5):66–78, 1991.
- [32] G. Singh, F. Mémoli, and G. Carlsson. [Topological methods for the analysis of high dimensional data sets and 3D object recognition](#). In *Eurograph. Sympos. Point-Based Graphics*, pages 91–100, 2007.
- [33] J. Tierny. *Reeb graph based 3D shape modeling and applications*. PhD thesis, Université des Sciences et Technologies de Lille, 2008.
- [34] J. H. van Lint and R. M. Wilson. *A course in Combinatorics*. Cambridge University Press, 1992.
- [35] Z. Wood, H. Hoppe, M. Desbrun, and P. Schröder. [Removing excess topology from isosurfaces](#). *ACM Trans. Graph.*, 23(2):190–208, 2004.
- [36] A. Zomorodian and G. Carlsson. [Computing persistent homology](#). *Discrete Comput. Geom.*, 33(2):249–274, 2005.